JASA ARTICLE

Environmental parameters sensitivity analysis for the modeling of wind turbine noise in downwind conditions

Bill Kayser,[1,a)] Benjamin Cotté,[2] David Ecotière,[3] and Benoit Gauvreau[1]

[1]*Unité Mixte de Recherche en Acoustique Environnementale, Université Gustave Eiffel, Cerema, Allée des Ponts et Chaussées Route de la Bouaye, 44340 Bouguenais, France*

[2]*Institut des Sciences de la Mécanique et Applications, École Nationale Supérieure de Techniques Avancées Paris, Centre National de la Recherche Scientifique, Commissariat à l'Énergie Atomique et aux Énergies Alternatives, Électricité de France, Institut Polytechnique Paris, Paris, France*

[3]*Unité Mixte de Recherche en Acoustique Environnementale, Cerema, Université Gustave Eiffel, 11, rue Jean Mentelin–Boîte Postale 9, 67035 Strasbourg, France*

ABSTRACT:

Modeling a wind turbine sound field involves taking into account the main aeroacoustic sources that are generally dominant for modern wind turbines, as well as environmental phenomena such as atmospheric conditions and ground properties that are variable in both time and space. A crucial step to obtain reliable predictions is to estimate the relative influence of environmental parameters on acoustic emission and propagation, in order to determine the parameters that induce the greatest variability on sound pressure level. Thus, this study proposes a Morris sensitivity analysis of a wind turbine noise emission model combined with a sound propagation model in downwind conditions. The emission model is based on Amiet's theory and propagation effects are modeled by the wide-angle parabolic equation. The whole simulation takes into account ground effects (absorption through acoustic impedance and scattering through surface roughness) and micrometeorological effects (mean refraction through the vertical gradient of effective sound speed). The final results show that the parameters involved in atmospheric refraction and in ground absorption have a significant influence on sound pressure level. On the other hand, in the context of this study the relative air humidity and the ground roughness parameters appear to be negligible on sound pressure level sensitivity.

 https://doi.org/10.1121/10.0002872

(Received 21 February 2020; revised 9 November 2020; accepted 13 November 2020; published online 11 December 2020)

[Editor: Michael J. White] Pages: 3623–3632

I. INTRODUCTION

Wind turbine sound emissions and propagation are affected by meteorological effects (e.g., vertical mean wind, temperature gradients, atmospheric turbulence) and ground effects (e.g., impedance, roughness, topography). As noise regulatory limitations constrain the installation of wind farms, it is crucial to estimate with reliability the dependence of sound pressure level (SPL) predictions on space and time. This requires accurate modeling of the aeroacoustic sources that are generally dominant for modern wind turbines (Bertagnolio *et al.*, 2017; Buck *et al.*, 2016; Oerlemans and Schepers, 2009), as well as the propagation effects. Indeed, the propagation phenomena fluctuate over highly variable time scales, from seasonal trends to instantaneous fluctuations, as well as over spatial scales, which lead to tremendous spread of SPL (Cheinet *et al.*, 2018; Gauvreau, 2013; Kayser *et al.*, 2018; Wilson, 2003; Zouboff *et al.*, 1994). Thus, an important step to obtain reliable prediction is to use statistical methods to quantify the model's sensitivities and uncertainties (Pettit and Wilson, 2007; Renterghem and Botteldooren, 2018; Wilson *et al.*, 2014).

Regarding wind turbine noise predictions, previous work focused mainly on ground effects (Kayser *et al.*, 2019) or on emission topics and/or atmospheric conditions impacts (Barlas *et al.*, 2017; Cotté, 2019; Heimann *et al.*, 2018; Lee *et al.*, 2016; McBride and Burdisso, 2017), but none of them considered the parameter sensitivity for the whole emission-propagation sound chain. The objective of this paper is to determine the influence of environmental parameters on wind turbine noise predictions in downwind conditions. These conditions usually represent the most detrimental conditions for the neighbourhood, as the SPL is significantly lower in upwind and crosswind conditions at long range (Barlas *et al.*, 2017). To do so, we propose to chain an extended aeroacoustic source model based on Amiet's theory (Roger and Moreau, 2010; Tian and Cotté, 2016) to a propagation model based on the wide-angle parabolic equation (WAPE) with the same approach as in Cotté (2019). This approach enables us to correctly predict both wind turbine noise emission and sound propagation.

[a)]Also at: UMRAE, Cerema, Université Gustave Eiffel, 11, rue Jean Mentelin–BP 9, 67035 Strasbourg, France. Electronic mail: bill.kayser@ifsttar.fr, ORCID: 0000-0002-3403-2540.

The sensitivity of the combined modeling of emission and propagation is estimated using the Morris screening method (Morris, 1991). This method allows one to determine the influence of the model input parameters on the model outputs (Saltelli *et al.*, 2000). First, the model performs calculations according to a design of experiment generated by the Morris algorithm. Second, the effects of each calculation on the model outputs are quantified by the method. Finally, sensitivity indices are calculated to determine the most influential parameters. The Morris method is called a screening method because it discretizes the inputs into several values called levels (Faivre *et al.*, 2013) and does not use the probability laws of the input parameters (Iooss, 2011). The main advantages are that it ranks the parameters according to their influence and that it identifies those that have nonlinear effects (e.g., interaction between parameters), while having a low calculation cost.

Section II of the paper reviews theories on the emission and propagation models, and explains the *chained* technique. The sensitivity analysis is presented in Sec. III, where the case study is detailed. The results are discussed for both medium and long range propagation cases in Sec. IV. Finally, Sec. V concludes and presents the perspectives.

II. DESCRIPTION OF CHAINED MODELS

A. Aeroacoustic emission model based on Amiet's theory

As proposed in Tian and Cotté (2016), the emission model is a trailing edge noise and turbulent inflow noise model for wind turbines based on Amiet's theory (Amiet, 1975, 1976; Roger and Moreau, 2010). For an airfoil of chord c and span L that is fixed relative to a far-field receiver, and for an aspect ratio L/c greater than about 3, the power spectral densities (PSD) of the acoustic pressure can be written in the general form

$$S_{pp}^{F}(\mathbf{x_R},\omega) = Lc^2\left(\frac{\omega}{c_0}\right)^2 A(\mathbf{x_R},U) \times \Pi\left(\mathbf{x_R},\frac{\omega}{U}\right)\left|\mathcal{I}\left(\mathbf{x_R},\frac{\omega}{U}\right)\right|^2, \quad (1)$$

where $\mathbf{x_R}$ is the position of the far-field receiver, ω is the angular frequency at the receiver, U is the inflow velocity, $c_0 = \sqrt{\gamma R T_0}$ is the speed of sound with γ the heat capacity ratio of air, R the specific gas constant of air, T_0 the ground surface temperature, A a coefficient that depends on $\mathbf{x_R}$ and U, Π a statistical function, and $\mathcal{I}$ an aeroacoustic transfer function. The superscript F refers to the *fixed* airfoil. The PSD of acoustic pressure is driven by the behavior of the functions Π and $\mathcal{I}$, which depend on the considered noise generation mechanism: turbulent inflow noise or trailing edge noise, as detailed in Roger and Moreau (2010) and Tian and Cotté (2016).

For a rotating blade at the angular position Φ (see Fig. 1), the PSD at a far-field receiver at an angular frequency ω is written (Sinayoko *et al.*, 2013; Tian and Cotté, 2016)

$$S_{pp}^{R}(\mathbf{x_R^T},\omega,\Phi) = \frac{\omega_e}{\omega} S_{pp}^{F}(\mathbf{x_R^B},\omega_e,\Phi), \quad (2)$$

where ω_e is the emission angular frequency, $\mathbf{x_R^T}$ the receiver coordinates in the wind turbine reference system, and $\mathbf{x_R^B}$ the receiver coordinates in the blade reference system. The superscript R refers to the *rotating* airfoil. The expression for the Doppler factor ω/ω_e is given in Sinayoko *et al.* (2013).

Since the incidence flow is not uniform along a wind turbine blade, a strip theory is used that consists of cutting each blade into D segments of variable chord c_d and span L_d, so as to respect the condition $L_d/c_d \geq 3, d = 1 \cdots D$, for which Eq. (1) is valid. Summation of the contributions from all blade segments is finally performed at the receiver by assuming that the different segments are uncorrelated (Tian and Cotté, 2016).

Since this analytical emission model is only valid in free field and homogeneous atmosphere, a propagation model is needed to account for ground and meteorological effects. The chained method between the Amiet emission model and a propagation model is presented below.

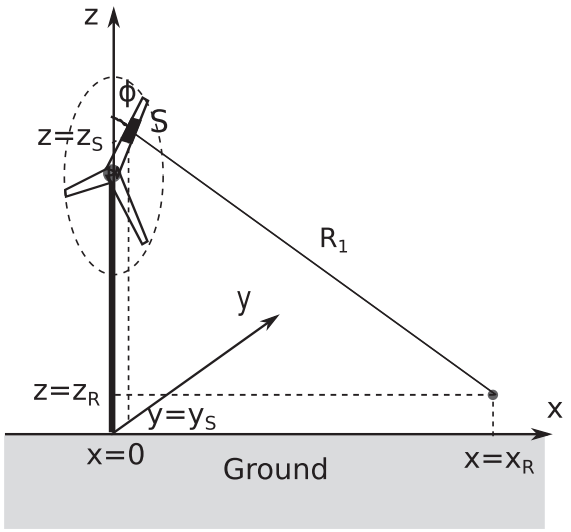

FIG. 1. Schematics of the moving monopoles approach with a receiver located at ($\mathbf{x_R}$,0, $\mathbf{z_R}$).

B. The moving monopoles approach

In the moving monopoles model that is detailed and validated in Cotté (2019), the SPL at the receiver is calculated for a blade segment S at an angular position Φ (see Fig. 1), using the point source approximation (Salomons, 2001):

$$\mathrm{SPL}(\omega,\Phi) = \overbrace{\mathrm{SWL}(\omega,\Phi}^{\text{emission}} \overbrace{-10\log(4\pi R_1^2)}^{\text{geometrical spreading}} \underbrace{+\Delta L(\omega,\Phi) - \alpha(\omega)R_1}_{\text{atmospheric and ground effects}}, \quad (3)$$

where $\mathrm{SWL}(\omega,\Phi)$ is the angle-dependent sound power level, $R_1 = \sqrt{\mathbf{x_R^2} + y_s^2 + (z_s - \mathbf{z_R})^2}$ is the distance between

https://doi.org/10.1121/10.0002872

the segment at $(0,y_s,z_s)$ and the receiver at $(\mathbf{x_R},0,\mathbf{x_R})$, ΔL is the sound attenuation relative to the free field, and α is the atmospheric absorption coefficient in dB/m. The angle-dependent $\mathrm{SWL}(\omega,\Phi)$ can be obtained from the free-field SPL calculated using Amiet's model (Cotté, 2019). The attenuation $\Delta L(\omega,\Phi)$ can be calculated using any propagation model that can take into account meteorological effect and ground effect. In this study we are using a propagation model based on the parabolic approximation of the wave equation (see Sec. II C). In order to limit the number of PE calculations to perform, a set of $N_h = 7$ fixed source heights H_n distributed along the rotor plane is considered,

$$H_n = H_{\min} + n\Delta H, \quad n = 0,\ldots,N_h - 1, \tag{4}$$

with ΔH the height step given by

$$\Delta H = \frac{H_{\max} - H_{\min}}{N_h - 1}, \tag{5}$$

where $H_{\min}$ and $H_{\max}$ are, respectively, the minimum height and the maximum height to consider. The attenuation $\Delta L(\omega,\Phi)$ is then obtained using the nearest-neighbor interpolation for the source height. The maximum difference between the fictive position of the source and the exact source height is thus $\Delta H/2$. This fictive position is only used to calculate the relative $\Delta L(\omega,\Phi)$, since the variables $\mathrm{SWL}(\omega,\Phi)$ and R_1 are calculated from the exact source positions.

C. Propagation model based on the parabolic equation approximation

As detailed in Kayser *et al.* (2019), the propagation model is a parabolic equation method with a numerical scheme based on high order Padé (2,2) approximants (Chevret *et al.*, 1996), and solved with the method of Collins (1993). The model assumes an inhomogeneous propagation medium, which implies that the real moving atmosphere is replaced by a hypothetical motionless medium with the effective sound speed $c_{\mathrm{eff}} = c_s + v_x$, where v_x is the wind velocity component along the direction of sound propagation and c_s the sound speed. The model is based on the WAPE derived from the Helmholtz elliptic equation for the sound pressure. The WAPE can be solved for the wave propagating in the positive x direction ($\delta = +1$) or negative x direction ($\delta = -1$),

$$\frac{\partial\phi(x,z)}{\partial x} = jk_0\delta(\mathcal{Q}_{pd} - 1)\phi(x,z), \tag{6}$$

where $\phi(x,z) = \sqrt{x}p_c e^{-j(\delta k_0 x)}$ is an envelope function which varies less rapidly with distance than the sought complex pressure p_c, $k_0 = \omega/c_0$ is the acoustic wave number, and $\mathcal{Q}_{pd}$ is a pseudo-differential operator whose square is defined as

$$\mathcal{Q}_{pd}^2 = \frac{1}{k^2}\frac{\partial^2}{\partial z^2} + n^2, \tag{7}$$

with $n = c_0/c_{\mathrm{eff}}$ the index of refraction.

The WAPE is solved at each spatial step, chosen here as $\lambda/20$ with λ the wavelength. As methods based on the parabolic equation can solve acoustic propagation problems above a mixed ground in a refractive and scattering atmosphere, it makes them particularly suitable and accurate for acoustic simulations in long-range outdoor sound propagation (Lihoreau *et al.*, 2006).

1. Ground effects

Acoustic properties of the ground (porous absorption and scattering by rough surface) are taken into account by an effective admittance model inspired by the work initially carried out in electromagnetism (Bass and Fuks, 1979). The implementation of this formulation in the parabolic equation model considered here has been validated and detailed in Kayser *et al.* (2019). The effective admittance β_{eff} is defined as follows:

$$\beta_{\mathrm{eff}} = \beta + \beta_{\mathrm{rough}} = \frac{1}{Z} + \beta_{\mathrm{rough}}, \tag{8}$$

where Z is the acoustic impedance of the ground and β_{rough} is the average effect of surface roughness on admittance. The impedance Z is described in this study by the Miki's impedance model (Miki, 1990)

$$\frac{Z}{Z_0} = 1 + 6.17\left(\frac{\rho_0 f}{a_{\mathrm{fr}}}\right)^{-0.632} + i9.44\left(\frac{\rho_0 f}{a_{\mathrm{fr}}}\right)^{-0.632}, \tag{9}$$

$$\frac{k}{k_0} = 1 + 8.73\left(\frac{\rho_0 f}{a_{\mathrm{fr}}}\right)^{-0.618} + i12.76\left(\frac{\rho_0 f}{a_{\mathrm{fr}}}\right)^{-0.618}, \tag{10}$$

where $Z_0 = \rho_0 c_0$ is the specific impedance of air, ρ_0 is the density of air, k is the wavenumber for sound waves in the ground, $f = \omega/2\pi$ is the frequency, and a_{fr} is the ground airflow resistivity (kN s m^{-4}). This model has a frequency validity range defined by the relation $f > 0.01\,a_{\mathrm{fr}}/\rho_0$ (Kirby, 2014) which is verified here.

The expression for β_{rough} corresponds to a 2D rough surface with a small and slowly varying roughness (Brelet and Bourlier, 2008), valid under the condition $|k_0\zeta\cos\theta_i| < 1$ and $|\partial\zeta/\partial x| < 1$, verified here, where ζ (m) is the roughness height profile of the ground and θ_i is the angle between the incident wave and the line perpendicular to the ground. The parameter β_{rough} is given by

$$\beta_{\mathrm{rough}}(\kappa) = \int_{-\infty}^{+\infty} \frac{\mathrm{d}\kappa'}{k_0 k_z(\kappa')}(k_0^2 - \kappa\kappa')W(\kappa - \kappa'), \tag{11}$$

with $\kappa = k_0\sin\theta_i$, where $k_z(\kappa) = \sqrt{k_0^2 - \kappa^2}$ and W is the roughness spectrum of the ground. The roughness spectrum is the Fourier transform of the autocorrelation function of the surface height profile. Considering that the probability density of the ground roughness heights is a normal distribution, W is defined as follows (Bourlier *et al.*, 2013):

$$W(k) = \frac{\sigma_h^2 l_c}{2\sqrt{\pi}} e^{-k^2 l_c^2/4}, \quad (12)$$

where σ_h is the standard deviation of the ground roughness heights and l_c the correlation length of the horizontal variations of the ground.

2. Atmospheric medium effects

In this study, the ground can present some roughness but the mean topography is considered as flat, so we assume that the atmosphere wind and temperature gradients are not dependent on horizontal range x. With this assumption it is then possible to neglect the evolution of the wind and temperature vertical profiles with distance due to the topography. The average vertical profile of effective celerity is then defined as follows:

$$\langle c_{\text{eff}}(z)\rangle = \sqrt{\gamma R \langle T(z)\rangle} + \langle U(z)\rangle \cos\theta, \quad (13)$$

with θ the angle between wind direction and sound propagation direction. $U(z)$ and $T(z)$ are the vertical wind speed and air temperature profiles, which are expressed as the sum of a mean part (in angle brackets) and a stochastic random part (indicated by primes),

$$U(z) = \langle U(z)\rangle + U'(z), \quad (14)$$

$$T(z) = \langle T(z)\rangle + T'(z). \quad (15)$$

The shapes of these micrometeorological profiles can be determined using different methods, such as the Monin-Obukhov similarity theory (Monin and Obukhov, 1954) or power laws, for example. In this study the micrometeorological flux is assumed to have logarithmic profiles defined as follows:

$$\langle U(z)\rangle = a_u \ln\left(\frac{z-d}{z_0}\right), \quad (16)$$

$$\langle T(z)\rangle = T_0 + a_T \ln\left(\frac{z-d}{z_0}\right), \quad (17)$$

where a_u (m s^{-1}) and a_T (K m^{-1}) are coefficients that determine the shape of the profiles (Gauvreau, 2013), $d = 0.66h_v$ is the displacement height accounting for the influence of vegetation height h_v (m) on the entire vertical profile, and $z_0 = 0.13h_v$ is the roughness height of the flux profiles (Brutsaert, 1982).

Moreover, atmospheric absorption is taken into account in the model in accordance with the ISO9613–1:1993 standard (ISO, 1993), which depends on air temperature T (K), atmospheric pressure p_{atm} (Pa), and the relative humidity of air h_r (%).

III. SENSITIVITY ANALYSIS OF ENVIRONMENTAL PARAMETERS

Sensitivity analysis is the study of the relative influence of different input parameters on the output. Usually, a model performs calculations according to a certain design of experiment (Monte Carlo sampling, Latin Hypercube sampling, etc.) in order to study its sensitivities. Then the effects of each calculation on the model output are quantified, and sensitivity indices are determined. Two main categories of design of experiment exist: one-at-a-time (OAT), which means that the value of a single parameter has changed between two calculations (this method does not take into account interactions between parameters), and full factorial designs which tests all possible combinations of parameters (it is often difficult to implement that method because of its high cost in terms of calculation time).

A. Morris method

As in Kayser *et al.* (2019), the Morris method (Morris, 1991; Saltelli *et al.*, 2000) is used because it overcomes the limitation of an OAT design, while keeping a cost that increases linearly with the number of input parameters. The Morris method consists of repeating n times an OAT plan (trajectory) randomly in the parameter space, where each input parameter interval is discretized into a suitable number of levels depending on the number n. This leads to $n(m+1)$ runs, where m is the number of input parameters and n is generally taken between 5 and 10 (Saltelli *et al.*, 2008; Faivre *et al.*, 2013). The method starts by sampling a set of initial values within the defined ranges of possible values for all input parameters and by calculating the subsequent model output. The second step changes the values of one parameter (all other inputs remaining at their initial values) and calculates the resulting change in model output compared to the first result. Then, the value of another parameter is changed and the resulting modification in the model outcome compared to the second run is calculated. This goes on until all input variables are changed. Figure 2 illustrates this method with $n = 2$ trajectories and $m = 2$ parameters.

Each repetition i ($i = 1 \ldots n$) of the design of experiment allows one to evaluate an elementary effect $E_j^{(i)}$ (between two successive calculations) caused by an input parameters X_j. The entire experimental design provides an $n-$ sample of effects for each parameter, from which the following sensitivity indices are derived and expressed:

- $\mu^* = (1/n)\sum_{i=1}^{n} |E_j^{(i)}|$, average of the absolute values of the effects,
- $\mu = (1/n)\sum_{i=1}^{n} E_j^{(i)}$, average of the values of the effects,
- $\sigma = \sqrt{[1/(n-1)]\sum_{i=1}^{n} (E_j^{(i)} - \mu)^2}$, standard deviation of the effects.

Thus, the larger μ^*, the more the parameter contributes to the spread of the output, because it means that the elementary effect $E_j^{(i)}$ is important. It is therefore an influential parameter. Compared to μ^*, the index μ can be positive or negative. Its sign indicates whether a given parameter tends to increase or decrease the model output. The value of the standard deviation σ is associated with nonlinear effects. This index is used to detect parameters involved in interactions with other parameters.

https://doi.org/10.1121/10.0002872

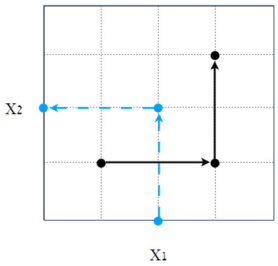

FIG. 2. (Color online) Illustration of Morris method with $n = 2$ trajectories represented by the dashed and solid arrows, and $m = 2$ parameters X_1 and X_2. The variation intervals of the parameters are discretized into five levels. The arrows represent the two different trajectories (the parameters values are modified during these trajectories), and the calculations are represented by the $n(m + 1) = 6$ points.

B. Case study

The case study is relative to the sound propagation of one wind turbine. The model output is the SPL averaged over one rotation [see Eq. (3)] expressed in dB, which leads to sensitivity indices also expressed in dB. The considered wind turbine has a nominal electrical power of 2.3 MW and a rotor diameter of 93 m. The hub height is 80 m and the three blades of 45 m length are decomposed into eight segments (Tian and Cotté, 2016). The rotational speed is supposed to increase linearly from 6 rpm at a cut-in wind speed of 4 m s^{-1} measured at the hub height, to 16 rpm at the rated wind speed of 12 m s^{-1}. As the studied physical phenomena depend on frequency, and considering the shape of the wind turbines sound source spectrum, we performed a sensitivity analysis at 14 different frequencies from 50 Hz to 1000 Hz. These frequencies correspond to the center frequencies of the 1/3-octave bands of this interval. The relative influence of the environmental parameters are quantified at three specific points in the calculation domain: (125, 0) m, (500, 2) m, and (1500, 2) m, which in the case of wind turbine noise can be considered respectively as close, medium, and long range propagation cases.

C. Parameters

This study focuses on downwind propagation conditions. The atmospheric turbulence is not taken into account because its influence on sound propagation is usually negligible for these conditions. Nevertheless, specific downwind conditions (θ close to 90°) combined with negative temperature gradients, see Eq. (13), can lead to the creation of shadow zone where turbulence can be significant. In order to avoid unrealistic SPL in the shadow zone in these rare situations [less than 8% for the (θ, a_u, a_T) combinations considered here], following Heimann and Salomons (2004) the turbulence is accounted by introducing a limit of $\Delta L \geq -25$ dB.

To illustrate the framework of this study regarding the atmospheric medium properties, Fig. 3 presents the minimum and maximum temperature, wind, and effective sound speed profiles that can be obtained with some combinations of the parameters. In order to build the design of experiment according to the Morris method (see Sec. III A), the number of trajectories is set to $n = 10$, and the variation intervals for the nine parameters are discretized into four values and are in Table I. The variation intervals of the ground parameters

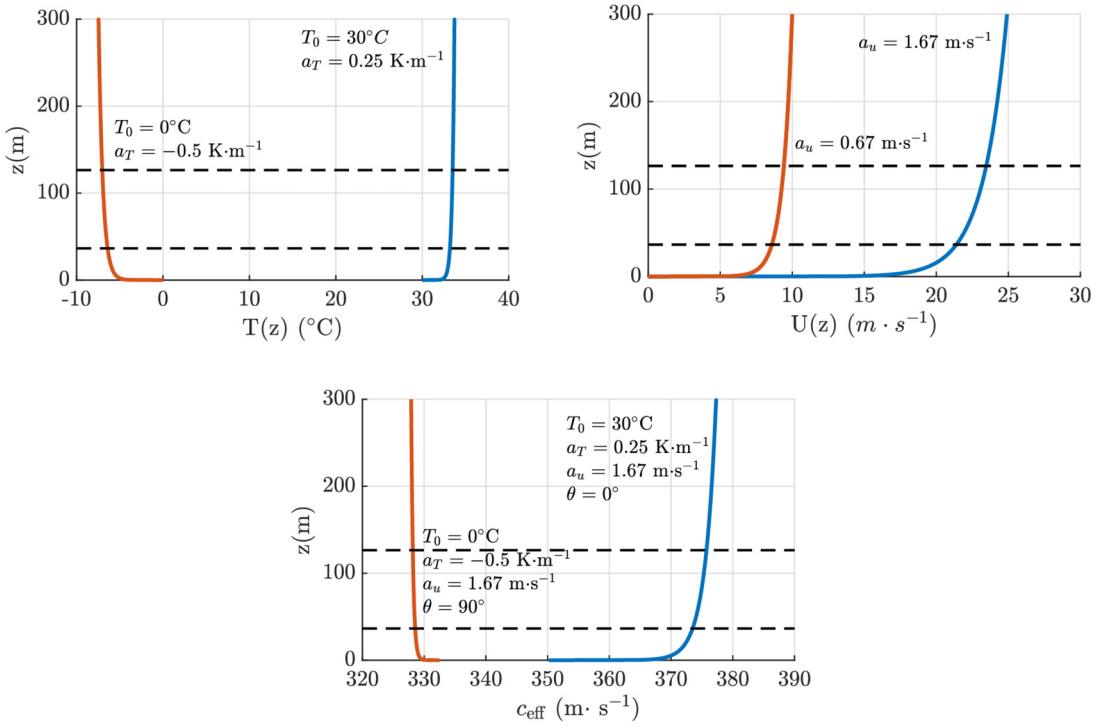

FIG. 3. (Color online) Minimum (red) and maximum (blue) vertical profiles of temperature, wind and effective sound speed for different combination of T_0, a_T, a_u, and θ parameters, for $h_v = 0$ m. The minimum and maximum heights of the rotor are represented by horizontal dashed lines.

TABLE I. Discretization of the variation intervals of the inputs parameters with four values for the Morris analysis.

Parameters	Description	Case 1	Case 2	Case 3	Case 4
a_{fr} (kN s m^{-4})	Airflow resistivity of the ground	50	500	1000	5000
l_c (m)	Correlation length of the rough ground	0.05	0.37	0.68	1
σ_h (m)	Standard deviation of the roughness Height	0.01	0.023	0.037	0.05
h_r (%)	Relative humidity of air	40	60	80	100
T_0 (°C)	Ground surface temperature	0	10	20	30
a_T (K m^{-1})	Temperature profile coefficient	−0.5	−0.25	0	0.25
a_u (m s^{-1})	Wind profile coefficient	0.67	0.98	1.33	1.67
h_v (m)	Vegetation height	0	0.33	0.66	1
θ (deg.)	Wind and source-receiver angle	0	30	60	90

(a_{fr}, l_c, and σ_h) are selected from values found in previous *in situ* experimental campaigns (Blaes and Defourny, 2008; Borgeaud and Bellini, 1998; Davidson *et al.*, 2000; Embleton *et al.*, 1983; Gauvreau, 2013; Nicolas and Berry, 1984). We focus on low vegetation heights so the h_v parameter has a maximum of 1 m. The h_r, T_0, and a_T parameters are representative average values for temperate climate. The values of the wind profile coefficient a_u are chosen to cover the entire operating range of the wind turbine. Regarding the angle θ between the wind and the source-receiver, we select cases between 0° and 90° so as not to induce upwind conditions.

IV. RESULTS

The results of the sensitivity analysis are discussed in three parts. Section IV A presents the parameters effects on emission. These results are obtained by setting $\Delta L(\omega, \Phi)$, $\alpha(\omega)$, and the geometrical spreading to zero in Eq. (3), with a modeled receiver located at (125, 0) m. Note that the modeled receiver location will induce an horizontal angle between the source and the modeled receiver. We verified that this angle does not bias the results of the analysis: the results are the same regardless of the modeled receiver position. Then, Sec. IV B shows the influence of the propagative effects on the SPL at the receiver by cancelling the $\mathrm{SWL}(\omega, \Phi)$ term in Eq. (3). Finally, Sec. IV C presents the total effects (emission + propagation).

A. Emission effects

Figure 4 shows the evolution of the 3 sensitivity indices of the Morris method (see Sec. III A) for the 9 parameters over the 14 frequencies. The wind profile coefficient a_u clearly appears as the main influential parameter (highest μ^* and μ) for all the frequencies considered, with a mean effect higher than 20 dB. This means that the emission sound levels vary on average by 20 dB when the wind coefficient a_u varies within the range defined in Table I. These results are consistent with the physics because the wind coefficient directly influences the wind speed, and so the rotational speed of the blades, which directly impacts the acoustic emission. The wind and source-receiver angle θ has a high influence on emission ($\mu^* > 10$ dB) in the [50; 250] Hz interval. Also, the index σ for the θ parameter is non negligible which indicates nonlinear effects; possibly interactions with other variables. This is presumably linked to the complex directivity of the wind turbine source that is influenced by the wind speed profile and by the angle between the wind and the source-receiver direction. The vegetation height h_v also emerges as an influential parameter with $\mu \approx -6$ dB for all the frequencies considered. This could be explained by the fact that the vegetation height induces a displacement height d on the meteorological profiles [see Eqs. (16) and (17)], and therefore influences the wind profile which is directly related to acoustic emission. When d increases the profiles are shifted upwards, thus the wind speed at the hub height decreases. This explains the μ negative values. Finally, the other six parameters (ground properties, ground surface temperature, temperature profile coefficient, and relative humidity) have zero μ^*, μ, and σ

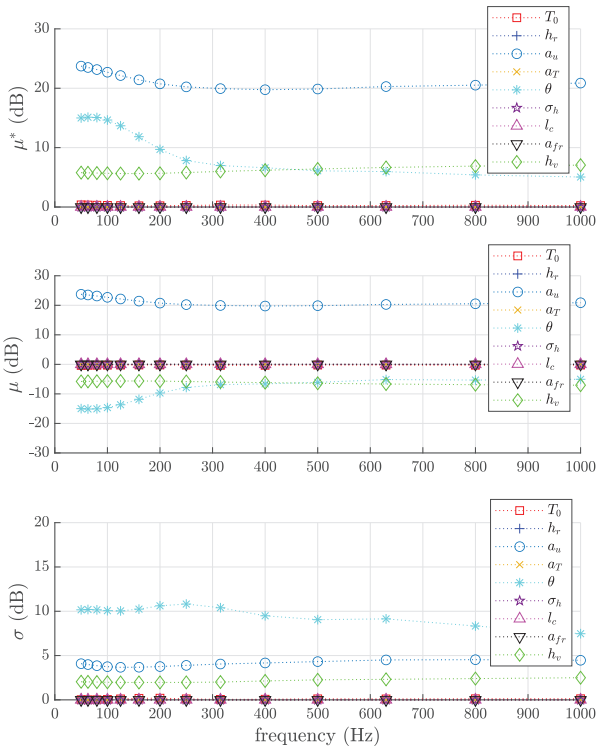

FIG. 4. (Color online) Values of the sensitivity indices μ^*, μ, and σ with respect to frequency for the nine varying environmental parameters considering only the emission effects.

https://doi.org/10.1121/10.0002872

values because they are not involved in the noise emission of the wind turbine.

B. Propagative effects

Figure 5 shows the values of the sensitivity indices μ^*, μ, and σ for propagative effects, at two receivers located, respectively, at (500,2) m and (1500,2) m using the same range of values as in Fig. 4.

The parameter with the highest influence on propagative effects (highest μ^* and σ for almost all frequencies) is the airflow resistivity of the ground a_{fr} which accounts for the ground absorption impedance. One can notice that the μ values for a_{fr} are fluctuating around 0, while its μ^* values are quite high (several dB). This reflects the fact that the variations of this parameter can induce an increase or decrease of the SPL, which tends to lower the value of the index μ. Then, it appears that the second most influential parameter is the angle between the wind and the source-receiver direction θ. Furthermore, the σ variations over frequency of the parameters a_{fr} and θ seem to be correlated. They follow the same trends, with maxima at the same frequency (200 Hz at 500 m and 250 Hz at 1500 m). It may indicate interactions between these two parameters. These interactions are certainly due to the influence of θ on refraction, which tends to modify the interference patterns due to ground effects.

At a distance of 500 m all the other parameters (T_0, h_r, a_u, a_T, σ_h, l_c, and h_v) have a lower influence on propagation, with an average $\mu^* \leq 1.5$ dB. However, the effects of many parameters (T_0, a_u, a_T, θ, a_{fr}, and h_v) are higher at the long range modeled receiver (1500 m) than at the modeled receiver located at (500 m). This is because the propagation effects are cumulative and increase with the distance. For example, we see that the influence of the wind gradient coefficient a_u and temperature gradient coefficient a_T emerge at 1500 m while they were negligible at 500 m. This can be explained by the atmospheric stratification that they induce, which affects sound propagation through refraction effects that increase with distance. The influence of the ground surface temperature T_0 is also non-negligible at 1500 m with μ^* values increasing from less than 0.5 dB at 100 Hz to $\mu^* \approx 2$ dB at 1000 Hz. This is undoubtedly related to its influence on the temperature gradient profile [see Eq. (17)], and on the atmospheric absorption effect. The vegetation height h_v also has a certain impact at 1500 m due to its influence on wind and temperature gradients that both affect refraction.

Finally, compared to the other parameters, the ground roughness parameters l_c and σ_h seem to have a marginal influence on the variation of sound levels considering that their μ^* values are close to 1 dB. It should be noted that these observations related to the influence of ground roughness are only valid in the context of this study on wind turbine noise, which considers a high altitude and extended sound source at frequencies lower than 1000 Hz. Indeed, other studies have shown the importance of ground roughness on acoustic propagation (Boulanger and Attenborough, 2005), even for a non-grazing sound source (Kayser *et al.*, 2019) when no meteorological effects take place. The relative humidity parameter h_r also has a very low μ^*. As relative humidity only plays a role in the atmospheric

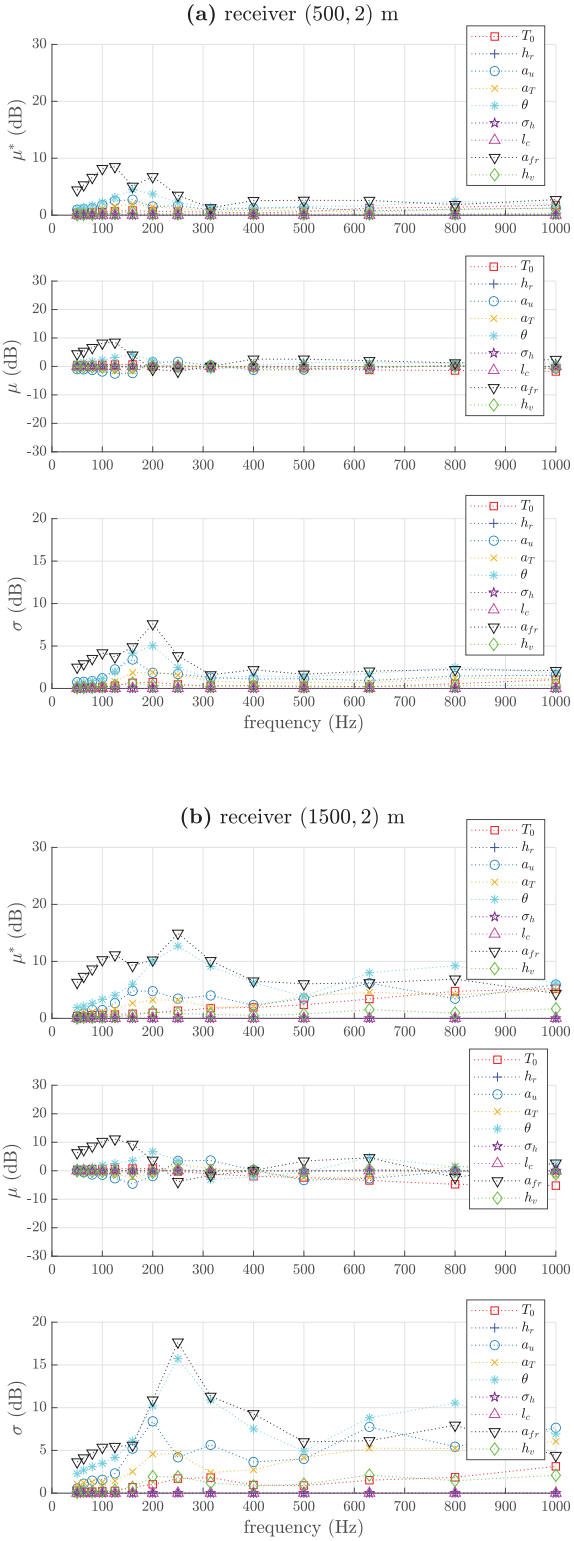

FIG. 5. (Color online) Values of the sensitivity indices μ^*, μ, and σ with respect to frequency for the nine varying environmental parameters, at two modeled receivers located at (500,2) m (a) and (1500,2) m (b). Only the propagative effects are considered here.

absorption calculation, which only has a significant impact at high frequencies, this result seems unsurprising given the frequency band considered here (50; 1000 Hz).

C. Combination of emission and propagative effects

Figure 6 presents the sensitivity indices for the total effects (emission + propagation) at the two modeled receivers located at (500,2) m and (1500,2) m. We first notice that the wind coefficient a_u is the most influential parameter for the total effects, with μ^* and μ values of about 20 dB for all the frequencies and receivers. This is because the wind gradient coefficient influences both noise emission and sound propagation as seen in Secs. IV A and IV B. The propagation angle θ and the vegetation height h_v parameters have important μ^* and μ values (several dB), which confirms that they are influential parameters. This is because they both play a role in the atmospheric flux profiles gradients (wind gradient for the propagation angle θ and wind and temperature gradients for the vegetation height h_v) that influence both noise emission and sound refraction. The airflow resistivity of the ground a_{fr} also has an important impact on total effects (several dB). It should be noted that the sensitivity indices of the airflow resistivity of the ground a_{fr} are exactly the same in between Figs. 5 and 6, because it only influences sound propagation. Likewise, the T_0, h_r, a_T, σ_h, l_c parameters only influence acoustic propagation and therefore show the same results between Figs. 5 and 6. Thus, as seen in Sec. IV B, the ground roughness parameters σ_h, l_c and the relative humidity of air h_r still have a negligible influence. Last, the nonlinear effects (index σ) of the different parameters are non-negligible at long range (1500 m), which confirms combined effects of atmospheric conditions and ground properties on SPL variability.

V. CONCLUSION

This study presents a Morris sensitivity analysis of a wind turbine noise emission and sound propagation model in order to determine the relative influence of environmental parameters on SPL variability in downwind conditions. The model used is composed of an aeroacoustics emission model based on Amiet's theory chained to a sound propagation model based on the parabolic equation. Atmospheric conditions are considered through six parameters: the wind and temperature profile coefficients a_u and a_T, the humidity of air h_r, the angle between the wind and the source-receiver directions θ, the vegetation height h_v, and the ground surface temperature T_0. Ground properties are taken into account through three parameters: the airflow resistivity of the ground a_{fr}, the standard deviation of the roughness height σ_h, and the correlation length of the rough ground l_c.

This study provides a quantitative classification of the parameters by order of influence for emission (Sec. IV A), propagation (Sec. IV B) and combined effects (emission + propagation) (Sec. IV C). Regarding the combined effects, the three parameters with the greatest sensitivities are the wind profile coefficient a_u, the angle between the wind and the source-receiver direction θ, and the airflow resistivity of the ground a_{fr}. The parameters with moderate influence are the temperature profile coefficient a_T, the vegetation height h_v, and the ground surface temperature T_0.

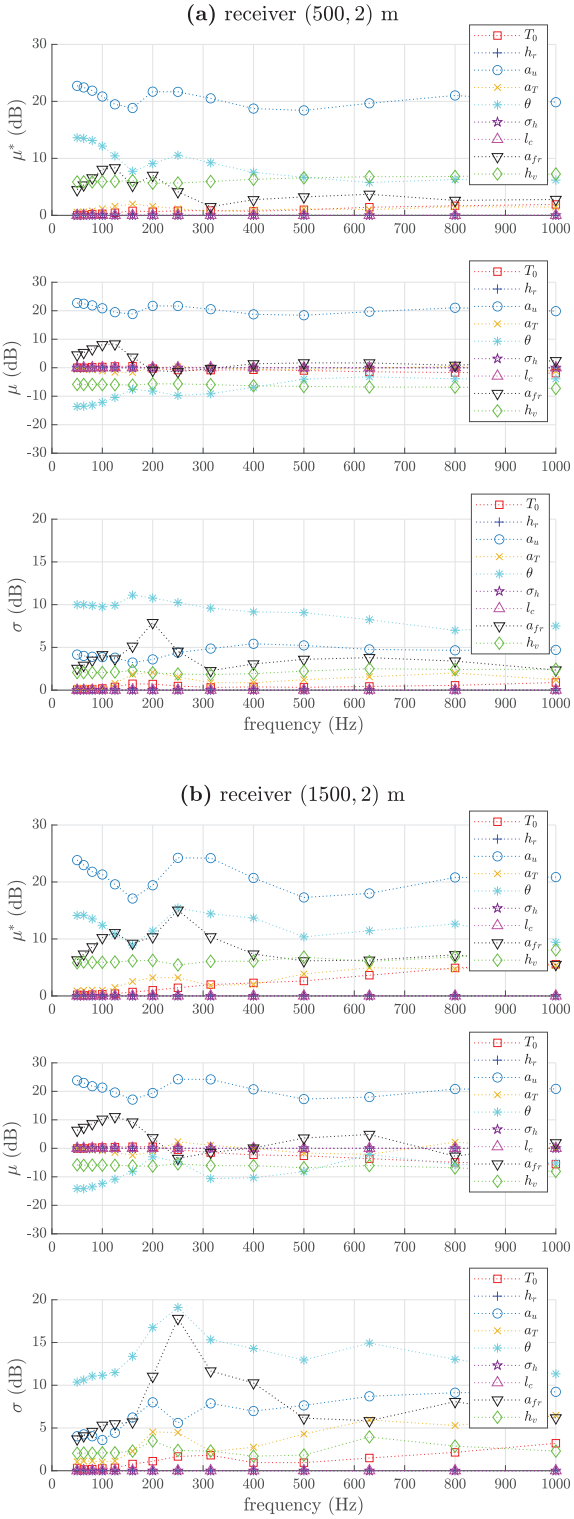

FIG. 6. (Color online) Values of the sensitivity indices μ^*, μ, and σ with respect to frequency for the nine varying environmental parameters, at two modeled receivers located at (500,2) m (a) and (1500,2) m (b). The total effects (emission and propagative effects) are considered here.

The parameters with low influence are the two ground roughness parameters (correlation length l_c and standard deviation of the roughness height σ_h) and the air humidity h_r. Even if relative humidity plays a certain role in atmospheric absorption, its influence is not visible here due to the considered frequency range: [50;1000] Hz. Although these sensitivities are mainly valid for this case study and could vary for another test configuration (for example, with a grazing point source and/or other receiver positions and/or other atmospheric conditions), the results provide useful information about the order of magnitude of several parameters' influence and on the possible interactions between parameters. These conclusions will help us to calculate uncertainties because it is then possible to "discard" non-influential parameters by considering them as constant, and so to reduce the complexity of the problem. Better knowledge of these variabilities will provide better control of wind turbine noise prediction quality in an inhomogeneous outdoor environment.

This study could be further improved by the consideration of atmospheric turbulence and by extending the analysis to upwind conditions because the shadow zones may feature distinct sensitivities. Also, it could be interesting to take into account several wind turbine sources to model a wind farm. Last, the results could be compared with *in situ* measurements in order to verify the variability range of the total SPL.

Amiet, R. K. (**1975**). "Acoustic radiation from an airfoil in a turbulent stream," J. Sound Vib. **41**(4), 407–420.
Amiet, R. K. (**1976**). "Noise due to turbulent flow past a trailing edge," J. Sound Vib. **47**(3), 387–393.
Barlas, E., Zhu, W. J., Shen, W. Z., Dag, K. O., and Moriarty, P. (**2017**). "Consistent modelling of wind turbine noise propagation from source to receiver," J. Acoust. Soc. Am. **142**(5), 3297–3310.
Bass, F. G., and Fuks, I. M. (**1979**). *Wave Scattering from Statistically Rough Surfaces: International Series in Natural Philosophy* (Elsevier, Amsterdam).
Bertagnolio, F., Madsen, H. A., and Fischer, A. (**2017**). "A combined aeroelastic-aeroacoustic model for wind turbine noise: Verification and analysis of field measurements," Wind Energy **20**(8), 1331–1348.
Blaes, X., and Defourny, P. (**2008**). "Characterizing bidimensional roughness of agricultural soil surfaces for SAR modeling," IEEE Trans. Geosci. Remote Sens. **46**(12), 4050–4061.
Borgeaud, M., and Bellini, A. (**1998**). "A database for electromagnetic scattering studies of bare soil surfaces," in *Proceedings of IGARSS '98, Sensing and Managing the Environment, 1998 IEEE International Geoscience and Remote Sensing*, Vol. 3, pp. 1197–1199.
Boulanger, P., and Attenborough, K. (**2005**). "Effective impedance spectra for predicting rough sea effects on atmospheric impulsive sounds," J. Acoust. Soc. Am. **117**(2), 751–762.
Bourlier, C., Pinel, N., and Kubické, G. (**2013**). *Method of Moments for 2D Scattering Problems: Basic Concepts and Applications* (Wiley, New York).
Brelet, Y., and Bourlier, C. (**2008**). "Bistatic scattering from a sea-like one-dimensional rough surface with the perturbation theory in HF-VHF band," in *Proceedings of IGARSS 2008, IEEE International Geoscience and Remote Sensing Symposium*, Vol. 4, pp. IV-1137–IV-1140.
Brutsaert, W. (**1982**). *Evaporation into the Atmosphere: Theory, History and Applications* (Springer, Dordrecht).
Buck, S., Oerlemans, S., and Palo, S. (**2016**). "Experimental characterization of turbulent inflow noise on a full-scale wind turbine," J. Sound Vib. **385**, 219–238.
Cheinet, S., Cosnefroy, M., Königstein, F., Rickert, W., Christoph, M., Collier, S. L., Dagallier, A., Ehrhardt, L., Ostashev, V. E., Stefanovic, A., Wessling, T., and Wilson, D. K. (**2018**). "An experimental study of the atmospheric-driven variability of impulse sounds," J. Acoust. Soc. Am. **144**(2), 822–840.
Chevret, P., Blanc-Benon, P., and Juvé, D. (**1996**). "A numerical model for sound propagation through a turbulent atmosphere near the ground," J. Acoust. Soc. Am. **100**(6), 3587–3599.
Collins, M. D. (**1993**). "A split-step Padé solution for the parabolic equation method," J. Acoust. Soc. Am. **93**(4), 1736–1742.
Cotté, B. (**2019**). "Extended source models for wind turbine noise propagation," J. Acoust. Soc. Am. **145**(3), 1363–1371.
Davidson, M. W. J., Toan, T. L., Mattia, F., Satalino, G., Manninen, T., and Borgeaud, M. (**2000**). "On the characterization of agricultural soil roughness for radar remote sensing studies," IEEE Trans. Geosci. Remote Sens. **38**(2), 630–640.
Embleton, T. F. W., Piercy, J. E., and Daigle, G. A. (**1983**). "Effective flow resistivity of ground surfaces determined by acoustical measurements," J. Acoust. Soc. Am. **74**(4), 1239–1244.
Faivre, R., Iooss, B., Mahévas, S., Makowski, D., and Monod, H. (**2013**). *Analyse de sensibilité et exploration de modèles: Application aux sciences de la nature et de l'environnement* (*Sensitivity Analysis and Model Exploration: Application to Natural and Environmental Sciences*) (Editions Quae, Versailles).
Gauvreau, B. (**2013**). "Long-term experimental database for environmental acoustics," Appl. Acoust. **74**(7), 958–967.
Heimann, D., Englberger, A., and Schady, A. (**2018**). "Sound propagation through the wake flow of a hilltop wind turbine-A numerical study," Wind Energy **21**(8), 650–662.
Heimann, D., and Salomons, E. M. (**2004**). "Testing meteorological classifications for the prediction of long-term average sound levels," Appl. Acoust. **65**(10), 925–950.
Iooss, B. (**2011**). "Revue sur l'analyse de sensibilité globale de modèles numériques" ("Review on global sensitivity analysis of numerical models"), J. Soc. Fran. Stat. **152**(1), 1–23.
ISO (**1993**). ISO9613-1:1993, "Acoustics—Sound attenuation in free field—Part 1: Atmospheric absorption calculation" (International Organization for Standardization, Geneva, Switzerland).
Kayser, B., Gauvreau, B., and Ecotière, D. (**2019**). "Sensitivity analysis of a parabolic equation model to ground impedance and surface roughness for wind turbine noise," J. Acoust. Soc. Am. **146**(5), 3222–3231.
Kayser, B., Gauvreau, B., Ecotière, D., and Le Bourdat, C. (**2018**). "A new experimental database for wind turbine noise propagation in an outdoor inhomogeneous medium," in *Proceedings of the 17th International Symposium on Long Range Sound Propagation*, Lyon, France.
Kirby, R. (**2014**). "On the modification of Delany and Bazley fomulae," Appl. Acoust. **86**, 47–49.
Lee, S., Lee, D., and Honhoff, S. (**2016**). "Prediction of far-field wind turbine noise propagation with parabolic equation," J. Acoust. Soc. Am. **140**(2), 767–778.
Lihoreau, B., Gauvreau, B., Bérengier, M., Blanc-Benon, P., and Calmet, I. (**2006**). "Outdoor sound propagation modeling in realistic environments: Application of coupled parabolic and atmospheric models," J. Acoust. Soc. Am. **120**(1), 110–119.
McBride, S., and Burdisso, R. (**2017**). "A comprehensive Hamiltonian ray tracing technique for wind turbine noise propagation under arbitrary weather conditions," in *Seventh International Meeting on Wind Turbine Noise*, pp. 1–12.
Miki, Y. (**1990**). "Acoustical properties of porous materials-Modifications of Delany-Bazley models," J. Acoust. Soc. Jpn. (E) **11**(1), 19–24.
Monin, A. S., and Obukhov, A. M. (**1954**). "Basic laws of turbulent mixing in the surface layer of the atmosphere," Contrib. Geophys. Inst. Acad. Sci. USSR **151**, 163–187.
Morris, M. D. (**1991**). "Factorial sampling plans for preliminary computational experiments," Technometrics **33**(2), 161–174.
Nicolas, J., and Berry, J. L. (**1984**). "Propagation du son et effet de sol" ("Sound propagation and ground effects"), Rev. Acoust. **71**(4), 191–200.
Oerlemans, S., and Schepers, J. G. (**2009**). "Prediction of wind turbine noise and validation against experiment," Int. J. Aeroacoust. **8**(6), 555–584.
Pettit, C. L., and Wilson, D. K. (**2007**). "Proper orthogonal decomposition and cluster weighted modeling for sensitivity analysis of sound propagation in the atmospheric surface layer," J. Acoust. Soc. Am. **122**(3), 1374–1390.
Renterghem, T. V., and Botteldooren, D. (**2018**). "Variability due to short-distance favorable sound propagation and its consequences for immission assessment," J. Acoust. Soc. Am. **143**(6), 3406–3417.

Roger, M., and Moreau, S. (**2010**). "Extensions and limitations of analytical airfoil broadband noise models," Int. J. Aeroacoust. **9**(3), 273–305.
Salomons, E. M. (**2001**). *Computational Atmospheric Acoustics* (Kluwer Academic, Dordrecht, the Netherlands).
Saltelli, A., Chan, K., and Scott, E. M. (**2000**). *Sensitivity Analysis* (Wiley, New York).
Saltelli, A., Ratto, M., Andres, T., Campolongo, F., Cariboni, J., Gatelli, D., Saisana, M., and Tarantola, S. (**2008**). *Global Sensitivity Analysis: The Primer* (Wiley, New York).
Sinayoko, S., Kingan, M., and Agarwal, A. (**2013**). "Trailing edge noise theory for rotating blades in uniform flow," Proc. R. Soc. A: Math. Phys. Eng. Sci. **469**(2157), 20130065.
Tian, Y., and Cotté, B. (**2016**). "Wind turbine noise modeling based on Amiet's theory: Effects of wind shear and atmospheric turbulence," Acta Acust. Acust. **102**(4), 626–639.
Wilson, D. K. (**2003**). "The sound-speed gradient and refraction in the near-ground atmosphere," J. Acoust. Soc. Am. **113**(2), 750–757.
Wilson, D. K., Pettit, C. L., Ostashev, V. E., and Vecherin, S. N. (**2014**). "Description and quantification of uncertainty in outdoor sound propagation calculations," J. Acoust. Soc. Am. **136**(3), 1013–1028.
Zouboff, V., Brunet, Y., Bérengier, M., and Sechet, E. (**1994**). "A qualitative approach of atmospheric effects on long range sound propagation," in *Proceedings of the 6th International Symposium on Long Range Sound Propagation*, Ottawa, Canada.